

Vapor–Liquid Equilibria and Saturated Liquid Densities in Binary Mixtures of Nitrogen, Methane, and Ethane and Their Correlation Using the VTPR and PSRK GCEOS

Jörg Janisch, Gabriele Raabe,* and Jürgen Köhler

Institut für Thermodynamik, Technische Universität Braunschweig, Hans-Sommer-Strasse 5, 38106 Braunschweig, Germany

New experimental data are presented for the vapor–liquid equilibria in the binary systems nitrogen + methane, nitrogen + ethane, and methane + ethane including data for the saturated liquid densities covering a temperature range of 130 K to 270 K and pressures up to 10.1 MPa. On the basis of the new experimental data for these binary mixtures, which may be regarded as model mixtures, the performance of the widely used group contribution equations of state VTPR and PSRK was investigated. These studies focused on the equations' ability to represent accurately saturated liquid densities over a wide range of temperatures and pressures when a constant volume translation was applied.

Introduction

The optimal design of separation processes requires accurate data for the phase equilibria to develop and evaluate reliable correlation models. However, even for assumed simple and well-studied systems such as mixtures of methane, ethane, and nitrogen, major components of natural gases, there are shortcomings regarding the availability of data in certain ranges of temperature, pressure, and composition and especially of data for saturated liquid densities. For that reason, comprehensive measurements of phase equilibria in mixtures of these components have been carried out in our laboratory. The experimental results for the vapor–liquid equilibria including saturated liquid densities for the binary systems of nitrogen, methane, and ethane are presented in this paper.

Enormous efforts are made to develop highly accurate reference equations of state for the correlation and prediction of phase equilibria, as, for example, the GERG equation for natural gas systems.¹ However, these models have been developed only for selected components, and determining properties of mixtures with other components not included in the models is impossible. For more general purposes, that is, the correlation of phase equilibria of arbitrary mixtures, cubic equations of state are still widely used in technical applications. Current work in this field is devoted to the further development of group contribution equations of state (GCEOS) such as PSRK^{2–4} and VTPR^{5–7} that link cubic equations of state with the UNIFAC model to get reliable predictive models with a wide range of applicability.

Especially the predictive Soave–Redlich–Kwong (PSRK) model that combines the SRK equation of state with UNIFAC by means of the PSRK g^E -mixing rule has become a very popular tool in the gas-processing industry. However, this model shows some weaknesses, especially regarding the description of saturated liquid densities.⁵ To overcome this shortcoming of the PSRK model, recent investigation of the Gmehling group dealt with the development of a new GCEOS, the VTPR model, that links the UNIFAC method by means of a modified mixing rule with a volume-translated Peng–Robinson EOS.

* Corresponding author. E-mail: G.Raabe@tu-bs.de.

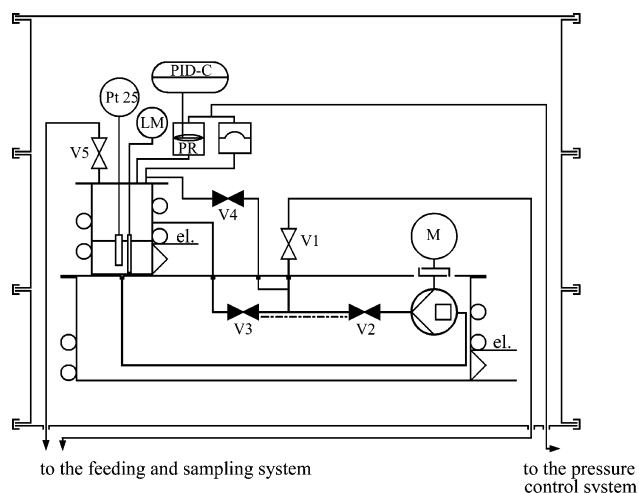


Figure 1. Schematic drawing of the VLE apparatus: the equilibrium cell is equipped with a Pt25 platinum resistance thermometer, a liquid level measuring (LM), and a differential pressure transducer (PR) that yields the signal of the PID controller (PID-C) in the pressure control system. The cooling coils with liquid nitrogen are connected with electric resistant heaters (el.).

Studies on the performance of the VTPR model have mainly focused on the description of the liquid densities of pure fluids. This is understandable due to the fact that experimental data for liquid saturated densities of mixtures are rare. With our new experimental results for the binary systems nitrogen + methane, methane + ethane, and nitrogen + ethane that can be regarded as model mixtures, we are able to investigate the VTPR GCEOS with respect to their ability to represent accurately saturated liquid densities over a wide range of pressures and temperatures.

However, the PSRK model is still further developed, and in their latest paper Horstmann et al.⁴ suggested the use of a volume translation for the PSRK model as well. Thus, we will also compare the predictions of the saturated liquid densities by a volume translated PSRK GCEOS (PSRK-VT) to the results of the VTPR model.

Table 1. Experimental Vapor–Liquid Equilibrium Data ($pTxy$) at Various Temperatures of the Mixture Nitrogen + Methane

T K	p MPa	x_{N_2}	y_{N_2}
130.029	0.5836	0.0425	0.3299
130.079	0.6137	0.0461	0.3468
149.989	2.9084	0.2774	0.5981
150.001	4.3871	0.5608	0.6990
149.928	4.5273	0.5938	0.6897
159.972	1.7892	0.0224	0.0908
159.989	3.6825	0.2659	0.4978
159.906	4.3027	0.3553	0.5390
160.000	4.6458	0.4156	0.5441
159.962	4.7291	0.4275	0.5465
169.983	3.9739	0.1700	0.3316
169.941	4.5058	0.2351	0.3746
170.018	4.8406	0.2845	0.3906
170.009	4.9334	0.3013	0.3919
169.935	4.9735	0.3248	0.3866
179.976	5.0615	0.1898	0.1930

Table 2. Experimental Data for the Saturated Liquid Densities ρ' of the VLE in the System Nitrogen + Methane

T K	p MPa	x_{N_2}	ρ' mol·L ⁻¹
129.982	1.5344	0.2952	23.1487
129.987	2.0732	0.4716	22.0853
149.972	2.0512	0.1389	21.5167
149.967	3.2093	0.3339	19.8395
149.958	3.6646	0.4151	18.8261
150.011	4.1123	0.5040	16.9512
150.001	4.3871	0.5608	15.5637
149.928	4.5273	0.5938	14.7656
159.982	1.7892	0.0224	20.5969
159.989	3.6825	0.2659	18.2392
159.361	4.0988	0.3238	17.5631
160.000	4.6458	0.4156	15.4385
159.962	4.7291	0.4275	15.2693
170.012	4.4385	0.2279	15.8115
169.984	4.5235	0.2384	15.5782
169.986	4.7183	0.2630	14.9957
170.009	4.9334	0.3013	13.6941
179.976	4.6722	0.1281	13.9515
179.976	5.0615	0.1898	11.3862

Table 3. Experimental Vapor–Liquid Equilibrium Data ($pTxy$) at Various Temperatures of the Mixture Nitrogen + Ethane

T K	p MPa	x_{N_2}	y_{N_2}
149.970	1.5788	0.0702	0.9886
149.973	3.1461	0.1469	0.9842
149.981	4.5509	0.2201	0.9872
170.039	0.5597	0.0184	0.9072
169.998	1.0116	0.0360	0.9494
169.948	1.0530	0.0370	0.9500
169.911	2.9932	0.1140	0.9724
169.873	5.0029	0.2041	0.9716
169.903	7.8543	0.3394	0.9562
209.927	1.1471	0.0236	0.6671
209.930	2.0607	0.0522	0.7866
210.022	3.0401	0.0810	0.8315
210.041	7.8831	0.2449	0.8713
210.012	9.9986	0.3312	0.8567
249.875	2.1789	0.0246	0.3257
249.983	3.1025	0.0518	0.4737
249.659	3.9349	0.0761	0.5533
250.027	6.0850	0.1483	0.6349
269.938	3.2681	0.0305	0.2308
270.013	4.1864	0.0600	0.3360
269.998	5.7557	0.1133	0.4299
269.907	8.0147	0.1969	0.4669

Experimental Section

A schematic drawing of the VLE apparatus used for our studies is shown in Figure 1. It consists of two main parts, the

Table 4. Experimental Data for the Saturated Liquid Densities ρ' of the VLE in the System Nitrogen + Ethane

T K	p MPa	x_{N_2}	ρ' mol·L ⁻¹
149.970	1.5788	0.0702	19.9243
169.998	1.0116	0.0360	18.7406
169.911	2.9932	0.1140	19.1883
169.873	5.0029	0.2041	19.4490
209.927	1.1471	0.0236	17.1238
210.043	10.0082	0.3352	17.2261
249.983	3.1025	0.0518	14.8017
249.659	3.9349	0.0761	14.8664
250.027	6.0850	0.1483	14.5616
269.938	3.2681	0.0305	13.5010
270.013	4.1864	0.0600	13.4340
269.907	8.0147	0.1969	12.5123
270.000	8.9229	0.2503	11.8678
269.967	10.1043	0.3581	10.1584

Table 5. Experimental Vapor–Liquid Equilibrium Data ($pTxy$) at Various Temperatures of the Mixture Methane + Ethane

T K	p MPa	x_{CH_4}	y_{CH_4}
139.984	0.4908	0.7327	0.9999
140.036	0.5000	0.7423	0.9999
140.016	0.6129	0.9408	0.9999
149.945	0.3916	0.3300	0.9865
149.960	0.5804	0.5170	0.9858
179.951	0.5253	0.1405	0.8395
179.926	1.0183	0.3005	0.9286
179.927	1.5182	0.4673	0.9546
180.056	1.5384	0.4731	0.9525
179.865	2.0381	0.6548	0.9696
179.931	2.3784	0.7678	0.9829
180.029	3.0216	0.9450	0.9960
209.878	2.0492	0.2898	0.8292
209.990	2.1397	0.3056	0.8331
209.954	3.0911	0.4597	0.8787
209.944	4.1298	0.6302	0.9073
209.949	5.0063	0.7653	0.9186
239.949	1.5239	0.0590	0.3476
240.001	4.4221	0.3679	0.7244
239.871	5.3739	0.4763	0.7504
240.041	5.4820	0.4880	0.7526
240.000	6.5669	0.6210	0.7472
270.058	2.8360	0.0504	0.1799
270.038	2.9075	0.0565	0.1994
270.010	4.2574	0.1717	0.3923
269.993	4.8145	0.2176	0.4363
270.032	5.8814	0.3143	0.4833
270.001	6.6263	0.4253	0.4493

equilibrium cell with the temperature and pressure measurement, and the circulation loop with the liquid sampling system. After equilibrium has been reached, a liquid sample can be separated in a sampling tube of well-known volume by closing the corresponding valves (V2, V3, and V4). The gas and the liquid sample are then withdrawn via V5 and V1. The liquid sample is weighed to enable the determination of the density of the liquid phase by $\rho' = (m/V)_{\text{sample}}$. Both samples are afterward analyzed by gas chromatography. The experimental uncertainties of the temperature and pressure measurements are $\Delta T = \pm 5$ mK and $\Delta p/p = 0.02$ % to 0.07 %. The molar compositions of the liquid and vapor phases are determined with an uncertainty of $\Delta x = \Delta y = 0.005$ mol·mol⁻¹. The uncertainties of the density measurements are estimated to be $\Delta \rho'/\rho' = \pm 0.4$ % to 0.9 %. A detailed description of this apparatus and the procedure of measurement is given in earlier papers.^{8–10} The results of our phase equilibrium measurements for the binary systems nitrogen + methane, nitrogen + ethane, and methane + ethane are listed in Tables 1 to 6 and plotted in Figures 2 to 7.

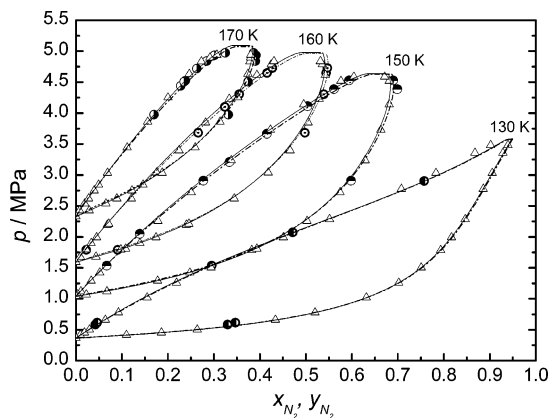


Figure 2. Vapor–liquid equilibria in the binary system nitrogen + methane: correlations by the VTPR (—) and PSRK (---) GCEOS in comparison with experimental data from this work (●, 130 K; ○, 150 K; ⊙, 160 K; ⊚, 170 K) and from Kidnay et al.¹⁵ (Δ).

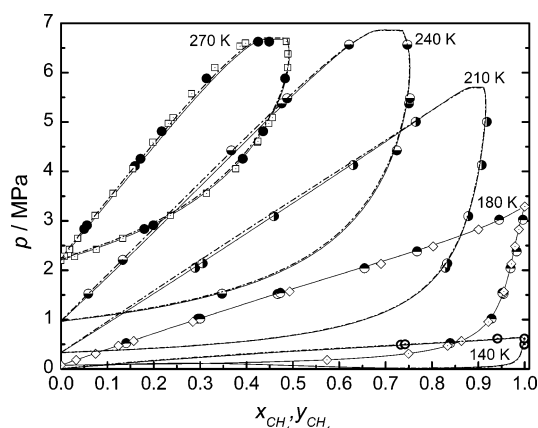


Figure 3. Vapor–liquid equilibria in the binary system methane + ethane: correlations by the VTPR (—) and PSRK (---) GCEOS in comparison with experimental data from this work (○, 140 K; ●, 180 K; ⊙, 210 K; ⊚, 240 K; ⊛, 270 K) and from the literature (◇, ref 23; □, ref 28).

Table 6. Experimental Data for Saturated Liquid Densities ρ' of the VLE in the System Methane + Ethane

T K	p MPa	x_{CH_4}	ρ' mol·L ⁻¹
139.984	0.4908	0.7327	22.8370
140.036	0.5000	0.7423	22.8729
140.016	0.6129	0.9408	23.2998
149.945	0.3916	0.3300	20.9835
179.832	1.0190	0.2964	19.1120
209.954	3.0911	0.4597	17.5299
209.949	5.0063	0.7653	15.7052
239.994	1.5239	0.0590	15.4216
239.865	2.2074	0.1336	15.5980
239.871	5.3739	0.4763	14.4644
240.000	6.5669	0.6210	12.4336
270.058	2.8360	0.0504	13.5827
269.974	4.1098	0.1596	13.1926
270.032	5.8814	0.3143	11.7676
270.001	6.6263	0.4253	9.1555

Thermodynamic Models

PSRK. The PSRK GCEOS is based on the Soave–Redlich–Kwong equation of state

$$p = \frac{RT}{v-b} - \frac{a}{(v+b)v} \quad (1)$$

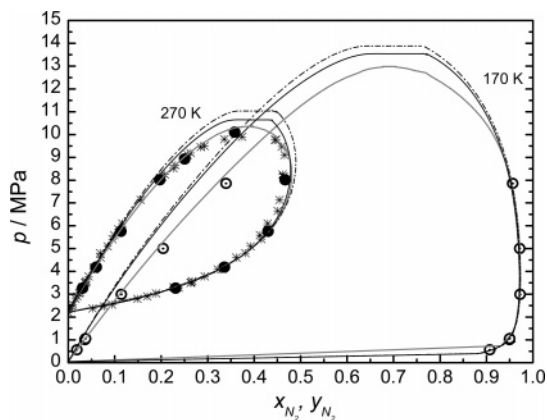


Figure 4. Vapor–liquid equilibria in the binary system nitrogen + ethane: predictions by the VTPR (—) and PSRK (---) GCEOS in comparison with experimental data from this work (○, 170 K; ●, 270 K) and from Gupta et al.²⁸ (*). Also shown are the results of the GERG reference equation (gray line, ref 1).

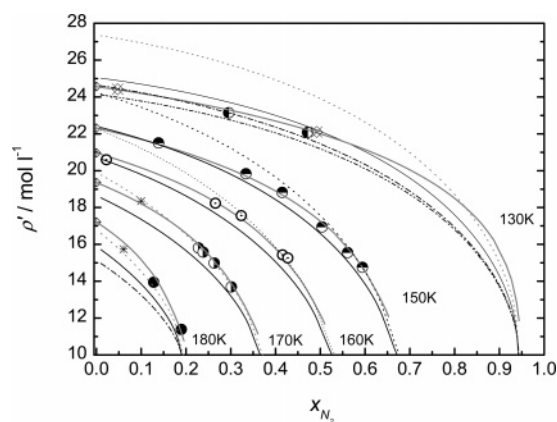


Figure 5. Saturated liquid densities in the binary system nitrogen + methane: predictions by the VTPR model (—), the (VT)PR model without volume translation (···), and PSRK (---, PSRK-VT; - · - ·, without volume translation) in comparison with experimental data from this work (●, 130 K; ○, 150 K; ⊙, 160 K; ⊚, 170 K; ⊛, 180 K) and from the literature (*, ref 16; crossed tilted square, ref 20). Also shown are the results of the GERG reference equation (gray line, ref 1) and experimental data for the saturated liquid densities of pure methane (crossed square, ref 35).

where the temperature function $\alpha_i(T)$ of the pure component parameter a_i

$$a_i(T) = 0.42748 \frac{R^2 T_{c,i}^2}{P_{c,i}} \alpha_i(T) \quad (2)$$

is expressed by the parameters $c_{1,i}$, $c_{2,i}$, and $c_{3,i}$

$$\alpha_i(T) = [1 + c_{1,i}(1 - \sqrt{T_{r,i}}) + c_{2,i}(1 - \sqrt{T_{r,i}})^2 + c_{3,i}(1 - \sqrt{T_{r,i}})^3]^2 \quad (3)$$

The parameters $c_{1,i}$, $c_{2,i}$, and $c_{3,i}$ of nitrogen, methane, and ethane have been fitted to experimental vapor pressure data and are given in ref 2.

To get a predictive GCEOS, the SRK EOS is combined with the UNIFAC model on the zero pressure reference state by the g^E -mixing rule PSRK

$$\frac{a}{b} = \sum_i x_i \frac{a_i}{b_i} + \frac{g_0^E}{A_{SRK}} + \frac{RT}{A_{SRK}} \sum_i x_i \ln \frac{b}{b_i} \quad A_{SRK} = -0.64663 \quad (4)$$

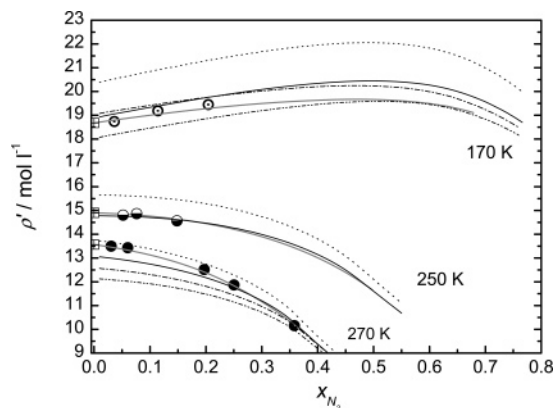


Figure 6. Saturated liquid densities in the binary system nitrogen + ethane: predictions by the VTPR (—) and (VT)PR model without volume translation (···), in comparison with PSRK (— · —, PSRK-VT; - · - ·, without volume translation) and experimental data from this work (○, 170 K; ●, 250 K; ●, 270 K). Also shown are the results of the GERG reference equation (gray line, ref 1) and experimental data for the saturated liquid densities of pure ethane (⊞, ref 34).

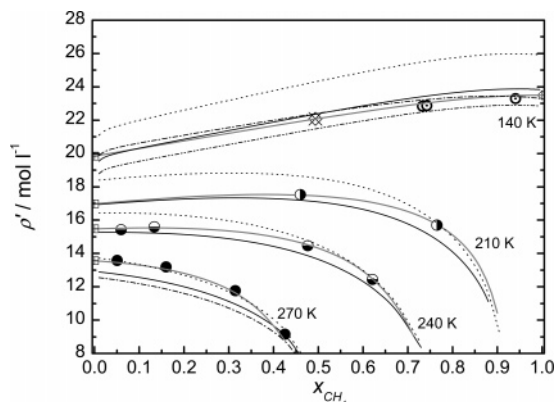


Figure 7. Saturated liquid densities in the binary system methane + ethane: predictions by the VTPR model (—), the (VT)PR model without volume translation (···), and PSRK (— · —, PSRK-VT; - · - ·, without volume translation) in comparison with experimental data from this work (○, 140 K; ●, 210 K; ●, 240 K; ●, 270 K) and from Hiza et al.²⁰ (crossed tilted square). Also shown are the results of the GERG reference equation (gray line, ref 1) and experimental data for the saturated liquid densities of pure ethane (⊞, ref 34), and pure methane (cross within tilted square, ref 35).

For the parameter b the classical linear mixing rule is employed:

$$b = \sum_i x_i b_i \quad (5)$$

New temperature-dependent group interaction parameters for the original UNIFAC main groups and new PSRK groups including gases such as CH_4 (57) and N_2 (60) have been established.^{2–4} Following the original UNIFAC concept, ethane is divided into two CH_3 groups to which the same interaction parameters are assigned as to a CH_2 group [CH_2 main group (1) parameters]. The interaction parameters for the group pairs 1 + 57, 1 + 60, and 57 + 60 used in this work are given in refs 2 and 3.

To improve the calculation of the liquid saturated densities, the Gmehling group suggests in ref 4 to employ the Péneloux volume translation¹¹ to the SRK EOS:

$$v = v_{\text{SRK}} - \sum_i x_i c_{i,\text{SRK}} \quad (6)$$

Table 7. Two α Parameters L , M , and N and Translation Parameter c for the VTPR and the PSRK EOS^a

component	VTPR parameters ⁶			c_i	$c_{i,\text{SRK}}$
	L	M	N	$\text{m}^3 \cdot \text{mol}^{-1}$	$\text{m}^3 \cdot \text{mol}^{-1}$
methane	0.94543	1.24525	0.42415	$4.33 \cdot 10^{-6}$	$8.403 \cdot 10^{-7}$
ethane	0.21225	0.87204	1.70100	$4.69 \cdot 10^{-6}$	$2.925 \cdot 10^{-6}$
nitrogen	$T > T_c$ for the systems considered here			$4.024 \cdot 10^{-6}$	$3.410 \cdot 10^{-7}$

^a Italicized values were determined in this work.

The constant translation parameters $c_{i,\text{SRK}}$ of the pure components can be either estimated from critical data

$$c_{i,\text{SRK}} = 0.40768 \frac{RT_{c,i}}{P_{c,i}} \left(0.29441 - \frac{P_{c,i} v_{c,i}}{RT_{c,i}} \right) \quad (7)$$

or determined from experimental liquid density.

VTPR. In the VTPR model, the Peng–Robinson EOS has been modified by introducing a translation parameter c to improve the description of liquid densities. Thus, the general expression of the VTPR equation of state^{5–7} is given by

$$p = \frac{RT}{v + c - b} - \frac{a}{(v + c)(v + c + b) + b(v + c - b)} \quad (8)$$

For each pure component, a constant parameter c_i is determined by the difference of the experimental and calculated densities at a reduced temperature of $T_r = 0.7$:

$$c = v_{\text{exptl}} - v_{\text{calcd}} \quad (9)$$

The c values for methane and ethane are given in ref 6. For nitrogen, no parameter c has been published by the Gmehling group so far. Thus, we determined c_{N_2} from the experimental data of Nowak et al.¹² Alternatively, the translation parameter can again be obtained from critical data by a generalized expression given in ref 6 or 7.

For the description of mixtures, a linear mixing rule for the parameter c is suggested.

Apart from the volume translation, the performance of the VTPR EOS is also improved by integration of the exponential temperature function $\alpha(T)$ by Twu et al.¹³ for the pure component parameter α :

$$\alpha(T) = T_r^{N(M-1)} \exp[L(1 - T_r^{NM})] \quad (10)$$

The values of the parameters N , M , and L for selected compounds including methane and ethane have been fitted to experimental vapor pressure data and are given in refs 6 and 7. Again, no parameters are available for nitrogen. However, in the systems studied in this work, nitrogen is supercritical. In this case (or if no parameters are available), $\alpha(T)$ is determined as a function of the acentric factor ω

$$\alpha(T) = \alpha^{(0)} + \omega(\alpha^{(1)} - \alpha^{(0)}) \quad (11)$$

The parameters $\alpha^{(0)}$ and $\alpha^{(1)}$ are calculated from eq 10 by using the generalized parameters for N , M , and L given in ref 6. The values of the parameters L , M , N , and c used in this work are summarized in Table 7.

A generalized GCEOS is again obtained by combining the VTPR EOS with the residual part of the UNIFAC model by

Table 8. Average Errors in Calculated Pressures and Vapor Compositions of the VTPR and PSRK Models^a

system	N_{exptl}	source: our work +	PSRK		VTPR		
			T	Δp	Δp	Δy	
			K	%	%	%	
$\text{N}_2 + \text{CH}_4$	392	refs 15–22	88 to 183	1.1	0.005	1.2	0.005
$\text{CH}_4 + \text{C}_2\text{H}_6$	297	refs 20, 23–28	111 to 283	3.7	0.008	2.2	0.006
$\text{N}_2 + \text{C}_2\text{H}_4$	177	refs 20, 28, 29–33	120 to 290	11.2	0.011	9.4	0.009

^a N_{exptl} refers to the number of experimental data considered that include our new experimental results and data from the literature.

means of a modified g^E -mixing rule This new mixing rule for the parameter a

$$\frac{a}{b} = \sum_i x_i \frac{a_{ii}}{b_{ii}} + \frac{g_{\text{res}}^A}{A_{\text{VTPR}}} \quad A_{\text{VTPR}} = -0.53087 \quad (12)$$

has been derived by simultaneously skipping the combinatorial part of the UNIFAC model and the Flory–Huggins term of the PSRK mixing rule (eq 4) to improve the prediction of asymmetric systems. Furthermore, a quadratic mixing rule for the parameter b is used with an exponent of $3/4$ for the binary parameter b_{ij} in the combination rule

$$b = \sum_i \sum_j x_i x_j b_{ij}, \quad b_{ij}^{3/4} = \frac{b_i^{3/4} + b_j^{3/4}}{2} \quad (13)$$

New temperature-dependent interaction parameters for the UNIFAC model have been fitted to vapor–liquid equilibrium data, excess enthalpies, and activity coefficients at infinite dilution.^{5–7,14} The group interaction parameters for the CH_2 main group (1) and methane (57) are given in ref 5; those for CH_2 (1) + N_2 (60) and CH_4 (57) + N_2 (60) are found in ref 14.

Results and Discussion

Prediction of the Vapor–Liquid Coexisting Curve. To compare the performances of the VTPR and PSRK models, we performed vapor–liquid equilibria calculations in the binary systems nitrogen + methane, nitrogen + ethane, and methane + ethane and determined the average errors in pressure

$$\Delta p/\% = \frac{1}{N} \sum_{i=1}^N \left| \frac{P_{\text{calcd},i} - P_{\text{exptl},i}}{P_{\text{exptl},i}} \right| \cdot 100 \quad (14)$$

and vapor compositions

$$\Delta y = \frac{1}{N} \sum_{i=1}^N \left| y_{\text{calcd},i} - y_{\text{exptl},i} \right| \quad (15)$$

for both GCEOS models for each binary system as summarized in Table 8. For this comparison, we considered not only our new experimental data but also data from the literature covering a wide range of temperatures and pressures. Table 8 also gives the number of experimental data points considered, their temperature range, and the references for the data from the literature. Experimental and calculated VLE of selected isotherms for the three binary systems are shown in the Figures 2 to 4. The figures also illustrate the good agreement of our new experimental results with data from the literature where they exist.

For the system nitrogen + methane both models yield very good results for the vapor–liquid phase equilibria with average errors of about $\Delta p = 1\%$. As shown in Figure 2, the original

PSRK model (depicted as a dash-dot line) gives pressures for this system that are slightly lower than those of the VTPR model (solid line), resulting in the better results. For the other binary systems investigated in this work, however, it is the other way round as shown by Figures 3 and 4. For the binary systems methane + ethane and nitrogen + ethane, the VTPR model yields lower pressures and with this a better reproduction of the phase equilibria.

Regarding the binary system nitrogen + ethane, Figure 4 reveals that both models have problems correlating correctly the vapor–liquid equilibria at lower temperatures. To make this clear, we plotted not only the correlations by the VTPR and PSRK models in comparison with experimental data but also the results of the GERG reference equation of state for natural gases¹, depicted as a bold gray line. As shown exemplarily by the depiction of the 170 K isotherm, both GCEOS models yield pressures that are much too high, with the VTPR model giving slightly lower pressures and therefore better results than the PSRK EOS. However, Figure 4 shows that the performance of both GCEOS is temperature dependent. For $T \leq 230$ K, both models show large deviations from experimental pressures with average errors of $\Delta p = 14.5\%$ (VTPR) and 16.8% (PSRK), whereas both GCEOS yield better results at higher temperatures ($T > 230$ K) with $\Delta p = 1.9\%$ for VTPR and $\Delta p = 3.3\%$ for PSRK. But also for these higher temperatures, the critical points are still overestimated by both models.

Prediction of Saturated Liquid Densities. The predictions of saturated liquid densities by the VTPR model and the PSRK-VT model employing constant volume translation parameters are investigated by determining the average errors between calculated and measured densities:

$$\Delta \rho' / \% = \frac{1}{N} \sum_{i=1}^N \left| \frac{\rho'_{\text{calcd},i} - \rho'_{\text{exptl},i}}{\rho'_{\text{exptl},i}} \right| \cdot 100 \quad (16)$$

These comparisons are based on our new experimental data and experimental results for saturated liquid densities from the literature.^{20,33} To investigate both the VTPR and PSRK models under the same conditions, we have not determined the translation parameters $c_{i,\text{SRK}}$ of the pure component from critical data by eq 7, but from experimental data for the liquid densities^{12,34,35} at $T_r = 0.7$ in the same way as it has been done for the VTPR model. The translation parameters for the PSRK-VT model are also given in Table 7. However, we have found that the differences in the predictions of saturated liquid densities by the PSRK-VT model with a translation parameter determined from experiment or from critical data are minor.

To investigate the improvement by the volume translation, we have also calculated saturated densities by the VTPR model with the translation parameter in eq 8 set to $c_i = 0$. The results of this predictive Peng–Robinson GCEOS without volume translation are identified by (VT)PR. For comparison, we have also determined the average errors for predicted saturated liquid densities of the PSRK model without and with employing a volume translation (PSRK-VT). The averaged errors in density are summarized in Table 9, again together with information on the number of data points considered, their temperature range, and references.

The predictions of the VTPR and PSRK models in comparison to experimental data for selected isotherms are plotted in Figures 5 to 7. As we focus our investigation regarding the calculation of liquid densities on the VTPR EOS, the predictions for this model, and for the corresponding model without volume translation (VT)PR, are shown for each isotherm (as solid and

Table 9. Average Errors in Calculated Liquid Densities of the VTPR and PRSK Model^a

system	N_{expt}	source: our work +	T	PSRK-VT	PSRK	VTPR	(VT)PR
			K	$\Delta\rho'$	$\Delta\rho'$	$\Delta\rho'$	$\Delta\rho'$
				%	%	%	%
N ₂ + CH ₄	40	refs 16, 20	105 to 180	3.3	3.6	2.1	8.3
CH ₄ + C ₂ H ₆	35	refs 20	105 to 270	2.4	4.8	1.9	7.2
N ₂ + C ₂ H ₆	25	refs 20, 33	105 to 270	3.5	4.7	2.3	8.5

^a PSRK-VT and VTPR apply a volume translation, whereas the translation parameter is set to $c_i = 0$ for PSRK and (VT)PR (no volume translation). N_{expt} refers to the number of experimental data considered that include our new experimental results and data from the literature.

dot lines, respectively). The results for the volume translated PSRK-VT model, however, are plotted only for a few isotherms (dash dot line). For clarification, we also show the results of the GERG reference equation of state for natural gases¹ (bold gray line) and reference data for the saturated liquid densities of the pure components.^{12,34,35}

In general, liquid densities are better described by the PR EOS than by the SRK EOS. Only for a few small spherical substances such as nitrogen or methane does the SRK model yield better results.⁵ Thus, without volume translation, the average error in saturated liquid densities in the system nitrogen + methane for the PSRK model is only $\Delta\rho' = 3.7\%$, whereas the (VT)PR model without volume translation yields much larger deviations from experiment. However, employing a constant translation parameter c remarkably reduces the average error of the VTPR model, whereas a volume translation does not significantly improve the performance of the PSRK-VT model. This is well illustrated by the depiction of the predicted saturated liquid densities of the 130 K isotherm in Figure 5.

For the system nitrogen + ethane, without volume translation, the PSRK model again gives a better reproduction of the experimental data than the (VT)PR EOS. This is due to the fact that the SRK EOS yields better results in the low-temperature range than the PR EOS, exemplarily shown for the 170 K isotherm in Figure 6. The volume translation noticeably reduces the deviations for the VTPR model mainly because of a better performance in the low-temperature range, so that it is then superior to the PRSK-VT model.

Corresponding results can be found for the binary system methane + ethane. For low temperatures, without volume translation, the PSRK model (dash-dot-dot line) is superior to the (VT)PR model (dot line), as shown in the depiction of the predicted saturated liquid densities for the 140 K isotherm in Figure 7. Applying a volume translation in the VTPR model (solid line) largely reduces the deviation in the low-temperature range. The performance of the volume translated PSRK-VT model, on the other hand, is not that much improved.

Thus, by employing a constant volume translation parameter c , the VTPR GCEOS better reproduces saturated liquid densities than the PSRK-VT with corresponding volume translation. However, Figures 5 to 8 reveal that the VTPR GCEOS yields increasing deviations from experiment with increasing temperature. Without volume translation, the (VT)PR model (dot line) significantly overpredicts the saturated liquid densities in all binary systems at lower temperatures. The use of the translation parameter reduces the predicted liquid densities and therefore gives results closer to the experimental data (solid line). With increasing temperature, the prediction of liquid densities by the (VT)PR EOS without volume translation improves and approaches the experimental data. Therefore, the volume translation results in an increasing underestimation of the densities. In the system nitrogen + methane, for example, the error in predicted densities for the VTPR model increases from $\Delta\rho' = 0.46\%$ for the temperature range $T < 150$ K to $\Delta\rho' = 4.9\%$

for higher temperatures. Ahlers and Gmehling⁵ have also investigated the use of a temperature-dependent volume correction (T-VTPR) to improve the reproduction of saturated liquid densities at higher temperatures, but decided against a further development of this idea, as it is well-known that empirical temperature-dependent volume translation can result in an unphysical crossing of the isotherms.^{36,37}

The volume translated PSRK-VT GCEOS yet shows similar deficiencies. The SRK EOS in general underestimates the liquid densities, and so employing a volume translation yields higher densities and a better reproduction of the experimental data. This is exemplarily shown by the 170 K isotherm in the system nitrogen + ethane in Figure 6. With increasing temperatures, the deviations from experiment also increase and cannot be compensated by a constant volume translation—as illustrated for the 270 K isotherm in Figure 6. Therefore, with increasing temperature, the PSRK-VT model with volume translation also yields increasing errors in the prediction of liquid densities, also with a growing underestimation of the experimental data. As for the system nitrogen + methane again, the average error in predicted densities rises from $\Delta\rho' = 1.3\%$ for $T < 150$ K to $\Delta\rho' = 6.2\%$ at higher temperatures.

Conclusion

We have reported new experimental data on the vapor–liquid equilibria in the binary systems nitrogen + methane, nitrogen + ethane, and methane + ethane including information on saturated liquid densities. On the basis of these new experimental results and available data from the literature, we investigated the performance of the group contribution equations of state VTPR and PSRK with regard to their reproduction of the vapor–liquid equilibria and, in particular, with respect to the prediction of saturated liquid densities.

Concerning the prediction of the vapor–liquid coexistence curves, the differences between both GCEOS are minor. Both models give reliable predictions of the vapor–liquid equilibria in the systems nitrogen + methane and methane + ethane with averaged errors in pressure between 1.1% and 3.7%. However, for the system nitrogen + ethane both VTPR and PSRK fail to reproduce accurately the phase equilibria in the lower temperature range.

Without the application of a volume translation, the PSRK model yields better results for the saturated liquid densities than the (VT)PR model due its advantages in systems with nitrogen and methane and a better reproduction of densities in the lower temperature range. The volume translation with a constant parameters c remarkably reduces the average error in liquid densities for the VTPR GCEOS, so it is then superior to the PSRK-VT model, for which the effect of a constant volume translation is not that pronounced. However, for both models with a constant volume translation, the deviations from experimental densities grow with increasing temperature, because of an increasing underestimation of the saturated liquid densities.

Literature Cited

- (1) Kunz, O.; Klimeck, R.; Wagner, W.; Jaeschke, M. *The GERG 2004 Wide-Range Reference Equation of State for Natural Gases and Other Mixtures*; To be published as GERG Technical Monograph. Fortschritt-Ber. VDI, VDI-Verlag: Düsseldorf, Germany, 2007.
- (2) Holderbaum, T.; Gmehling, J. PSRK: A Group Contribution Equation of State based on UNIFAC. *Fluid Phase Equilib.* **1991**, *70*, 251–265.
- (3) Fischer, K.; Gmehling, J. Further development. Status and results of the PSRK method for the prediction of vapor-liquid equilibria and gas solubilities. *Fluid Phase Equilib.* **1996**, *121*, 185–206.
- (4) Horstmann, S.; Jabloniec, A.; Krafczyk, J.; Fischer, K.; Gmehling, J. PSRK: group contribution equation of state: comprehensive revision and extension IV, including critical constants and α -function parameters for 1000 components. *Fluid Phase Equilib.* **2005**, *227*, 157–164.
- (5) Ahlers, J.; Gmehling, J. Development of a universal group contribution equation of state I. Prediction of liquid densities for pure compounds with a volume translated Peng–Robinson equation of state. *Fluid Phase Equilib.* **2001**, *191*, 177–188.
- (6) Ahlers, J.; Gmehling, J. Development of a Universal Group Contribution Equation of State II. Prediction of Vapor-Liquid Equilibria for Asymmetric Systems. *Ind. Eng. Chem. Res.* **2002**, *41*, 3489–3498.
- (7) Ahlers, J.; Gmehling, J. Development of a Universal Group Contribution Equation of State III. Prediction of Vapor-Liquid Equilibria, Excess Enthalpies, and Activity Coefficients at Infinite Dilution with the VTPR Model. *Ind. Eng. Chem. Res.* **2002**, *41*, 5890–5899.
- (8) Schulze, W. Phasengleichgewichte in asymmetrischen Gemischen aus Helium, Stickstoff und Methan. Ph.D. Thesis, TU Braunschweig, 1996.
- (9) Schulze, W. Vapor-liquid equilibria and saturation densities in the ternary system helium–nitrogen–methane. *Fluid Phase Equilib.* **1997**, *134*, 213–224.
- (10) Raabe, G.; Janisch, J.; Köhler, J. Experimental studies of phase equilibria in mixtures relevant for the description of natural gases. *Fluid Phase Equilib.* **2001**, *185*, 199–208.
- (11) Peneloux, A.; Rauzy, E.; Freze, R. A Consistent Correction for Redlich–Kwong–Soave Volumes. *Fluid Phase Equilib.* **1982**, *8*, 7–23.
- (12) Nowak, P.; Kleinrahm, R.; Wagner, W. Measurement and correlation of the (p , ρ , T) relation of nitrogen II. Saturated-liquid and saturated-vapour densities and vapour pressure along the entire coexistence curve. *J. Chem. Thermodyn.* **1997**, *29*, 1157–1174.
- (13) Twu, C. H.; Bluck, D.; Cunningham, J. R.; Coon, J. E. A Cubic Equation of State with a New Alpha Function and a New Mixing Rule. *Fluid Phase Equilib.* **1991**, *69*, 33.
- (14) Gmehling, J. AIF-report VTPR, Abschlussbericht 13885 N 2006, personal communication, 2007.
- (15) Kidnay, A. J.; Miller, R. C.; Parrish, W. R.; Hiza, M. J. Liquid–vapour phase equilibria in the N_2 – CH_4 system from 130 to 180 K. *Cryogenics* **1975**, *15*, 531–540.
- (16) Bloomer, O. T.; Parent, J. D. Liquid–vapor phase behavior of the methane–nitrogen system. *Chem. Eng. Prog. Symp. Ser.* **1953**, *49*, 11–24.
- (17) Parrish, W. R.; Hiza, M. J. Liquid–vapor equilibria in the nitrogen–methane system between 95 and 120 K. *Adv. Cryog. Eng.* **1974**, *19*, 300–308.
- (18) Stryjek, R.; Chappellear, P. S.; Kobayashi, R. Low-temperature vapor–liquid equilibria of nitrogen–methane system. *J. Chem. Eng. Data* **1974**, *19*, 334–339.
- (19) McClure, D. W.; Lewis, K. L.; Miller, R. C.; Staveley, L. A. K. Excess enthalpies and Gibbs free energies for nitrogen + methane at temperatures below the critical point of nitrogen. *J. Chem. Thermodyn.* **1989**, *8*, 785–792.
- (20) Hiza, M. J.; Haynes, W. M.; Parrish, W. R. Orthobaric liquid densities and excess volumes for binary mixtures of low molar-mass alkanes and nitrogen between 105 and 140 K. *J. Chem. Thermodyn.* **1977**, *9*, 873–896.
- (21) Kremer, H. Experimentelle Untersuchung und Berechnung von Hochdruck-Flüssigkeits-Dampf- und Flüssigkeits-Flüssigkeits-Dampf-Gleichgewichte für tiefsiedende Gemische. Ph.D. Thesis, TU Berlin, 1982.
- (22) Brandt, L. W.; Stroud, L. Phase equilibria in natural gas systems. Apparatus with windowed cell for 800 P.S.I.G. and temperatures to -320°F . *Ind. Eng. Chem.* **1958**, *50*, 849–852.
- (23) Miller, R. C.; Kidnay, A. J.; Hiza, M. J. Liquid + vapor equilibria in methane + ethene and in methane + ethane from 150.00 to 190.00 K. *J. Chem. Thermodyn.* **1977**, *9*, 167–178.
- (24) Wichterle, I.; Kobayashi, R. Vapor–liquid equilibrium of the methane–ethane system at low temperatures and high pressures. *J. Chem. Eng. Data* **1972**, *17*, 9–12.
- (25) Davalos, J.; Anderson, W. R.; Phelps, R. E.; Kidnay, A. J. Liquid–vapor equilibria at 250.00 K for systems containing methane, ethane, and carbon dioxide. *J. Chem. Eng. Data* **1976**, *21*, 81–84.
- (26) Price, A. R.; Kobayashi, R. Low temperature vapor–liquid equilibrium in light hydrocarbon mixtures: methane–ethane–propane system. *J. Chem. Eng. Data* **1959**, *4*, 40–52.
- (27) Miller, R. C.; Staveley, L. A. K. Excess enthalpies for some binary mixtures of low-molecular-weight alkanes. *Adv. Cryog. Eng.* **1976**, *21*, 493–500.
- (28) Gupta, M. K.; Gardner, G. C.; Hegarty, M. J.; Kidnay, A. J. Liquid–vapor equilibria for the $N_2 + CH_4 + C_2H_6$ system from 260 to 280 K. *J. Chem. Eng. Data* **1980**, *25*, 313–318.
- (29) Grauso, L.; Fredenslund, A.; Mollerup, J. Vapor–liquid equilibrium for the systems $C_2H_6 + N_2$, $C_2H_4 + N_2$, $C_3H_8 + N_2$, and $C_3H_6 + N_2$. *Fluid Phase Equilib.* **1977**, *1*, 13–26.
- (30) Stryjek, R.; Chappellear, P. S.; Kobayashi, R. Low-temperature vapor–liquid equilibria of nitrogen–ethane system. *J. Chem. Eng. Data* **1974**, *19*, 340–343.
- (31) Brown, T. S.; Sloan, E. D.; Kidnay, A. J. Vapor–liquid equilibria in the nitrogen + carbon dioxide + ethane system. *Fluid Phase Equilib.* **1989**, *53*, 7–14.
- (32) Kremer, H.; Knapp, H. Three-phase conditions are predictable. *Hydrocarbon Process.* **1983**, 79–83.
- (33) Raabe, G.; Köhler, J. Phase equilibria in the system nitrogen–ethane and their prediction using cubic equation of state with different types of mixing rules. *Fluid Phase Equilib.* **2004**, *222–223*, 3–9.
- (34) Funke, M.; Kleinrahm, R.; Wagner, W. Measurement and correlation of the (p , ρ , T) relation of ethane II. Saturated-liquid and saturated-vapour densities and vapour pressure along the entire coexistence curve. *J. Chem. Thermodyn.* **2002**, *34*, 2017–2039.
- (35) Kleinrahm, R.; Wagner, W. Measurement and correlation of the equilibrium liquid and vapour densities and the vapour pressure along the coexistence curve of methane. *J. Chem. Thermodyn.* **1986**, *18*, 739–760.
- (36) Yelash, L. V.; Kraska, T. Volume-Translated Equation of State: Empirical Approach and Physical Relevance. *AIChE J.* **2003**, *49* (6), 1569–1579.
- (37) Pfohl, O. Evaluation of an improved volume translation for the prediction of hydrocarbon volumetric properties. Letter to the editor. *Fluid Phase Equilib.* **1999**, *163*, 157–159.

Received for review April 24, 2007. Accepted June 19, 2007.

JE700210N